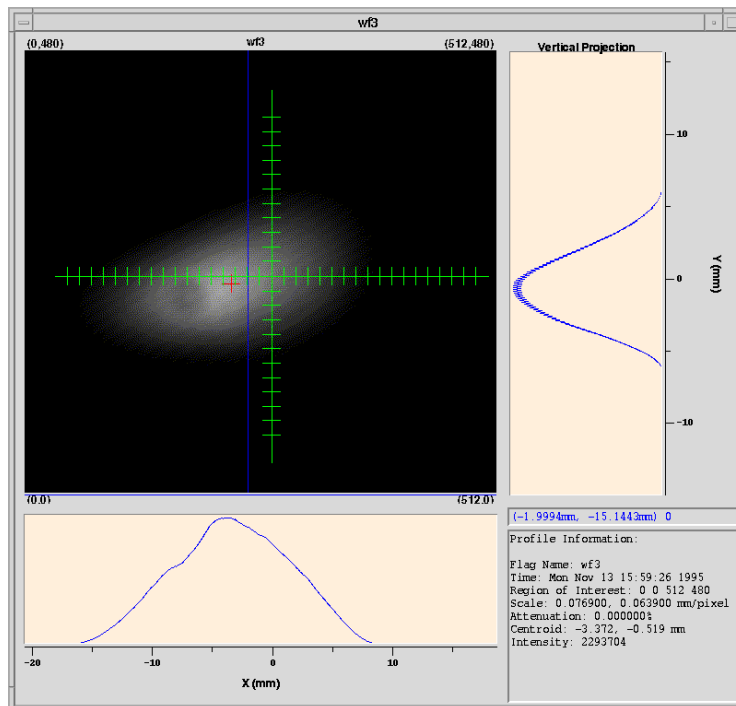


## Exercises:

### LINACS/Transport Lines Emittance Measurement



by Kay Wittenburg, -DESY-

## LINACS/Transport Lines Emittance Measurement

In a transfer line (or Linac), the beam passes once and the shape of the emittance ellipse at the entry to the line determines its shape at the exit. Exactly the *same* transfer line injected first with one emittance ellipse and then different ellipses has to be accredited with *different*  $\alpha$  and  $\beta$ ,  $\gamma$  functions to describe the cases. Thus  $\alpha$  and  $\beta$ ,  $\gamma$  depend on the input beam and their propagation depends on the structure. Any change in the structure will only change the  $\alpha$  and  $\beta$ ,  $\gamma$  values downstream of that point. ... The input ellipse must be chosen by the designer and should describe the configuration of all the particles in the beam.

### 1) Explain ways of measuring the emittance of a charged particle beam in a Linear accelerator or a transport line without knowing the beam optic parameters a, b, g.

- a) Exercise L1: Which one is the preferable method for a high energy proton transport line ( $p > 5$  GeV/c)?
- b) Exercise L2: Assuming that the geometry between the measurement stations and the transport matrices  $M$  of the transport line are well defined (including magnetic elements), describe a way to get the emittance using the  $\sigma$ -matrix.

$$\mathbf{s} = \begin{pmatrix} \mathbf{s}_{11} & \mathbf{s}_{12} \\ \mathbf{s}_{21} & \mathbf{s}_{22} \end{pmatrix} = \begin{pmatrix} \mathbf{s}_y^2 & \mathbf{s}_{yy} \\ \mathbf{s}_{yy} & \mathbf{s}_y^2 \end{pmatrix} = \mathbf{e}_{rms} \begin{pmatrix} \mathbf{b} & -\mathbf{a} \\ -\mathbf{a} & \mathbf{g} \end{pmatrix} = \mathbf{s} \text{ matrix}$$

- c) Exercise L3: In a transport line for  $p = 7.5$  GeV/c protons are two measurement stations. The first is located exactly in the waist of the beam and shows a beam width of  $\sigma_y = 3$  mm, the second at a distance of  $s = 10$  m shows a width of  $\sigma_y = 9$  mm. Assuming no optical elements in this part, calculate the emittance and the normalized emittance of the beam.

## References

S.Y. Lee, Accelerator Physics, World Scientific, pp 54-55 is attached

Emittance Measurements at the Bates Linac

*K.D. Jacobs, J.B. Flanz, T. Russ*

[http://accelconf.web.cern.ch/accelconf/p89/PDF/PAC1989\\_1529.PDF](http://accelconf.web.cern.ch/accelconf/p89/PDF/PAC1989_1529.PDF)

attached

Basic accelerator course, like Schmüser and Rossbach in previous CAS CERN 94-01 v 1

<http://doc.cern.ch/cgi-bin/tiff2pdf?/archive/cernrep/1994/94-01/p17.tif>

**Beam-line instruments/ [Raich, U](#) ;**

*In:* Joint US-CERN-Japan-Russia Particle Accelerators School on Beam Measurement, Montreux, Switzerland, 11-20 May 1998 - World Sci., Singapore, 1999. - pp.263-276

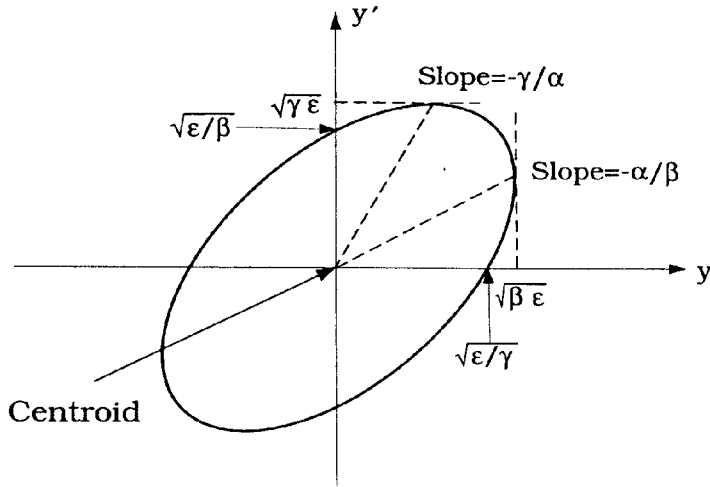


Figure 2.8: The Courant–Snyder invariant ellipse. The area enclosed by the ellipse is equal to  $\pi\epsilon$ , where  $\epsilon$  is twice the betatron action;  $\alpha, \beta$  and  $\gamma$  are betatron amplitude functions.

### A. The emittance of a beam

A beam is usually composed of particles distributed in the phase space. Depending on the initial beam preparation, we approximate a realistic beam distribution function by some simple analytic formula. Neglecting dissipation and diffusion processes, each particle in the distribution function has its invariant Courant–Snyder ellipse.

Given a normalized distribution function  $\rho(y, y')$  with  $\int \rho(y, y') dy dy' = 1$ , the moments of the beam distribution are

$$\langle y \rangle = \int y \rho(y, y') dy dy', \quad \langle y' \rangle = \int y' \rho(y, y') dy dy', \quad (2.94)$$

$$\sigma_y^2 = \int (y - \langle y \rangle)^2 \rho(y, y') dy dy', \quad \sigma_{y'}^2 = \int (y' - \langle y' \rangle)^2 \rho(y, y') dy dy', \quad (2.95)$$

$$\sigma_{yy'} = \int (y - \langle y \rangle)(y' - \langle y' \rangle) \rho(y, y') dy dy' = r \sigma_y \sigma_{y'}, \quad (2.96)$$

where  $\sigma_y$  and  $\sigma_{y'}$  are the rms beam widths,  $\sigma_{yy'}$  is the correlation, and  $r$  is the correlation coefficient. The rms beam emittance is then defined as

$$\epsilon_{\text{rms}} = \sqrt{\sigma_y^2 \sigma_{y'}^2 - \sigma_{yy'}^2} = \sigma_y \sigma_{y'} \sqrt{1 - r^2}. \quad (2.97)$$

If the accelerator is composed of linear elements such as dipoles and quadrupoles, the emittance defined in Eq. (2.97) is invariant. The rms emittance is equal to the phase-space area enclosed by the Courant–Snyder ellipse of the rms particle (see Exercise 2.2.16).

Although incorrect, the term “emittance” is often loosely used as twice the action variable of betatron oscillations. The betatron oscillations of “a particle” with an “emittance”  $\epsilon$  is

$$y(s) = \sqrt{\frac{\beta\epsilon}{\pi}} \cos[\nu\phi(s) + \delta]. \quad (2.98)$$

Figure 2.8 shows a Courant–Snyder invariant ellipse for a given emittance of a beam. For a beam with rms emittance  $\epsilon$ , the rms beam width is  $\sqrt{\beta(s)}\epsilon$ , and the beam rms divergence  $y'$  is  $\sqrt{\gamma(s)}\epsilon$ . Since  $\gamma = (1 + \alpha^2)/\beta$ , the transverse beam divergence is smaller at a location with a large  $\beta(s)$  value, i.e. all particles travel in parallel paths. In accelerator design, a proper  $\beta(s)$  value is therefore important for achieving many desirable properties.

### B. The $\sigma$ -matrix

The  $\sigma$ -matrix of a beam distribution is defined as

$$\sigma = \begin{pmatrix} \sigma_{11} & \sigma_{12} \\ \sigma_{12} & \sigma_{22} \end{pmatrix} = \begin{pmatrix} \sigma_y^2 & \sigma_{yy'} \\ \sigma_{yy'} & \sigma_{y'}^2 \end{pmatrix} = \langle (\mathbf{y} - \langle \mathbf{y} \rangle)(\mathbf{y} - \langle \mathbf{y} \rangle)^\dagger \rangle, \quad (2.99)$$

where  $\mathbf{y}$  is the betatron state matrix of Eq. (2.36),  $\mathbf{y}^\dagger = (y, y')$  is the transpose of  $\mathbf{y}$ , and  $\langle \mathbf{y} \rangle$  is the first moment. The rms emittance becomes (see also Exercise 2.2.14)

$$\epsilon_{\text{rms}} = \sqrt{\det \sigma} = \sqrt{\sigma_{11}\sigma_{22} - \sigma_{12}^2}. \quad (2.97)$$

Using the transfer matrix, we obtain

$$\sigma_2 = M_{21}\sigma_1 M_{21}^\dagger. \quad (2.100)$$

It is easy to verify that  $\mathbf{y}^\dagger \sigma^{-1} \mathbf{y}$  is invariant under linear betatron motion, thus the beam distribution is

$$\rho(y, y') = \rho(\mathbf{y}^\dagger \sigma^{-1} \mathbf{y}). \quad (2.101)$$

### C. Emittance measurement

The emittance can be obtained by measuring the  $\sigma$ -matrix. The beam profile of protons and ions is usually measured by using wire scanners or ionization profile monitors. Synchrotron light monitors are commonly used in electron storage rings. More recently, laser light has been used to measure electron beam size in the sub-micron range. Using the rms beam size and Courant-Snyder parameters, we can deduce the emittance of the beam.

## EMITTANCE MEASUREMENTS AT THE BATES LINAC\*

K. D. Jacobs, J. B. Flanz, and T. Russ.  
MIT Bates Linear Accelerator Center  
P.O. Box 846, Middleton, MA 01949

### Abstract

An emittance measuring system has been installed at the Bates Linear Accelerator Center. The system consists of three wire scanners used to measure the electron beam profile, plus a microcomputer for data acquisition and processing. The scanners are located in a drift space on a beam line. Each scanner measures the horizontal and vertical beam size with a possible resolution of  $25\ \mu\text{m}$ . The horizontal and vertical beam phase spaces can then be determined. Results of measurements are presented here. Calculations relating the theoretical accuracy of the emittance measurements with the distance separating the scanners, and the location and size of the beam waist, are also presented.

Another technique for measuring emittance has also been employed. This technique involves using a wire scanner to measure the beam size at a fixed location, as a function of the strength of an upstream quadrupole.<sup>1</sup>

### Introduction

The transverse phase space of a particle beam can be characterized by three parameters. For example, knowing the extent of the beam phase ellipse in distance and in angle, plus the orientation of the ellipse, will fully determine the phase space. An equivalent set of parameters is the location of a beam waist, the waist radius, and the maximum particle divergence at the waist. Various techniques can be used to measure these parameters. Measuring the beam size at three different locations, with fixed machine optics, will determine the phase space,<sup>2</sup> as will measuring the beam size at one location for three different optics configurations.

In this paper, we describe the technique for measuring the beam phase space by using the measurements of the beam sizes at three different locations. Calculations regarding the precision of this technique are presented, as are results of experimental measurements of the beam phase space at the Bates Linac.

### Measurement Technique

Consider a beam in a field free region (drift space). If  $x_0$  is the horizontal beam size at a waist located at axial position  $z_0$ , and  $\theta_0$  is the maximum horizontal divergence angle any particle makes with the beam axis at the waist, then the beam size  $x$  at location  $z$  is given by

$$x^2 = x_0^2 + (z - z_0)^2 \theta_0^2 \quad (1)$$

To measure the beam phase space, we measure the beam size using three profile monitors, equally spaced by the distance  $L$ . Defining the origin to be at the center profile monitor, so that  $z_1 = -L$ ,  $z_2 = 0$ , and  $z_3 = +L$ , the beam sizes  $x_i$  at the monitors are given by

$$\begin{aligned} x_1^2 &= x_0^2 + (L + z_0)^2 \theta_0^2 \\ x_2^2 &= x_0^2 + z_0^2 \theta_0^2 \\ x_3^2 &= x_0^2 + (L - z_0)^2 \theta_0^2 \end{aligned} \quad (2)$$

Thus, knowing the beam sizes  $x_i$  and the profile monitor separation  $L$ , we can calculate the waist size

$$x_0 = \left\{ x_2^2 - \frac{1}{8} \left( \frac{x_1^2 - x_3^2}{x_1^2 - 2x_2^2 + x_3^2} \right) \right\}^{1/2}, \quad (3)$$

the divergence at the waist

$$\theta_0 = \frac{1}{\sqrt{2}L} (x_1^2 - 2x_2^2 + x_3^2)^{1/2}, \quad (4)$$

and the location of the waist

$$z_0 = \frac{L}{2} \left( \frac{x_1^2 - x_3^2}{x_1^2 - 2x_2^2 + x_3^2} \right). \quad (5)$$

The particle beam emittance  $\epsilon$  is given by the product  $x_0 \theta_0$ ,

$$\epsilon = \frac{1}{4L} [8x_2^2(x_1^2 - 2x_2^2 + x_3^2) - (x_1^2 - x_3^2)^2]^{1/2}. \quad (6)$$

A similar set of calculations holds in the vertical dimension.

These calculations are for the case of equally spaced profile monitors in a drift space. They can be extended to include unequal monitor spacing and the presence of intervening optical components.

### Measurement Error Analysis

In order to make meaningful emittance measurements using beam profile monitors of realistic resolution, it may be necessary to set up the beam and the profile monitors in a particular manner. The precision of the measurements depends on  $L$ ,  $x_0$ , and  $z_0$ . (For a beam of fixed emittance,  $\theta_0 \propto x_0^{-1}$ , and is not an independent variable.) In general, the precision of an emittance measurement increases with increasing  $L$ , and when the waist is located closer to the center profile monitor.

To quantitatively determine the uncertainty in the phase space measurements, standard propagation of error calculations have been made. In making these calculations, it has been assumed that the uncertainty in the measured beam sizes  $\sigma_{x_i}$  dominate, and that  $L$  is known to greater precision. The results are

$$\begin{aligned} \frac{\sigma_{x_0}}{x_0} &= \left\{ \sigma_{x_1}^2 x_1^2 (x_1^2 - x_3^2)^2 (x_1^2 - 4x_2^2 + 3x_3^2)^2 \right. \\ &\quad + 4\sigma_{x_2}^2 x_2^2 [4(x_1^2 - 2x_2^2 + x_3^2)^2 - (x_1^2 - x_3^2)^2]^2 \\ &\quad \left. + \sigma_{x_3}^2 x_3^2 (x_1^2 - x_3^2)^2 (3x_1^2 - 4x_2^2 + x_3^2)^2 \right\}^{1/2} \\ &\quad / 4\sqrt{2}x_0^2 (x_1^2 - 2x_2^2 + x_3^2)^2, \end{aligned} \quad (7)$$

$$\frac{\sigma_{\theta_0}}{\theta_0} = \sqrt{2} \frac{(\sigma_{x_1}^2 x_1^2 + 4\sigma_{x_2}^2 x_2^2 + \sigma_{x_3}^2 x_3^2)^{1/2}}{(x_1^2 - 2x_2^2 + x_3^2)}, \quad (8)$$

$$\begin{aligned} \sigma_{z_0} &= \frac{2L}{(x_1^2 - 2x_2^2 + x_3^2)^2} [\sigma_{x_1}^2 x_1^2 (x_2^2 - x_3^2)^2 \\ &\quad + \sigma_{x_2}^2 x_2^2 (x_1^2 - x_3^2)^2 + \sigma_{x_3}^2 x_3^2 (x_1^2 - x_2^2)^2]^{1/2}, \end{aligned} \quad (9)$$

\* Work supported by the U.S. Department of Energy

and

$$\frac{\sigma_\epsilon}{\epsilon} = \frac{4}{\sqrt{2}[8x_2^2(x_1^2 - 2x_2^2 + x_3^2) - (x_1^2 - x_3^2)^2]} \times [\sigma_{x_1}^2 x_1^2 (x_1^2 - 4x_2^2 - x_3^2)^2 + 16\sigma_{x_2}^2 x_2^2 (x_1^2 - 4x_2^2 + x_3^2)^2 + \sigma_{x_3}^2 x_3^2 (x_1^2 + 4x_2^2 - x_3^2)^2]^{1/2}. \quad (10)$$

Using Eq. (10), the beam configuration for making optimum emittance measurements can be found. For example, the effect of moving the location of the beam waist is shown in Fig. 1, for fixed monitor separation and different waist sizes.

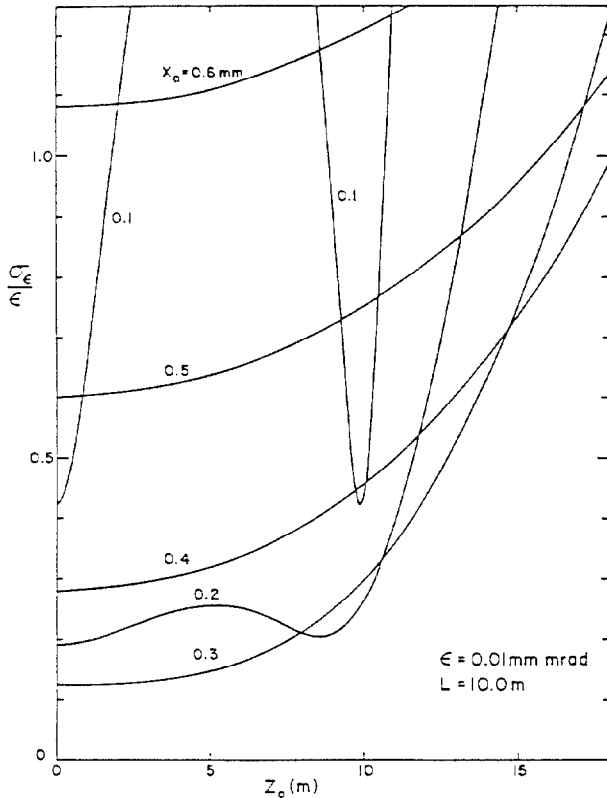


Fig. 1: Precision of emittance measurement  $\sigma_\epsilon$  vs. location of waist  $z_0$ , for different waist sizes  $x_0$ . Here  $L = 10$  m and  $\epsilon = 0.01$  mm · mrad. The precision of the beam width at each profile monitor is taken to be  $\sigma_{x_i} = 25$   $\mu$ m.

As can be seen, it is always best to have the waist near the center monitor ( $z = 0$ ), although for some  $x_0$  this requirement is not as critical. (When  $z_0 \approx 0$ , the precision of  $x_0$  is improved, which leads to a decrease in  $\sigma_\epsilon$ .) Figure 1 also indicates that for fixed  $z_0$ , there is a dependency of  $\sigma_\epsilon$  on  $x_0$ . This is shown explicitly in Fig. 2, which plots  $\sigma_\epsilon$  as a function of  $x_0$  for  $z_0 = 0$ , and several different  $L$ . The optimum value of  $x_0$  as a function of  $L$  is shown in Fig. 3. Finally, with  $x_0$  at its optimum value and  $z_0 = 0$ , the obtainable  $\sigma_\epsilon$  is shown as a function of  $L$  in Fig. 4. Here we see that the obtainable fractional precision  $\sigma_\epsilon/\epsilon$  scales as  $L^{-1/2}$ .

### Experimental Results

Emittance measurements at Bates, based on the above analysis, are made with an automatic emittance measuring system. The beam profiles are determined using high resolution wire scanners.<sup>3</sup> Data from the scanners are digitized, acquired,

and processed by the Linac Control System. The processing is done on a MicroVAX by programs written in a high level language, and includes fitting a Gaussian to the profile data to determine the beam size. Once the size is known at each scanner, the emittance, beam waist size and location, and beam divergence are calculated, along with estimates of their uncertainties.

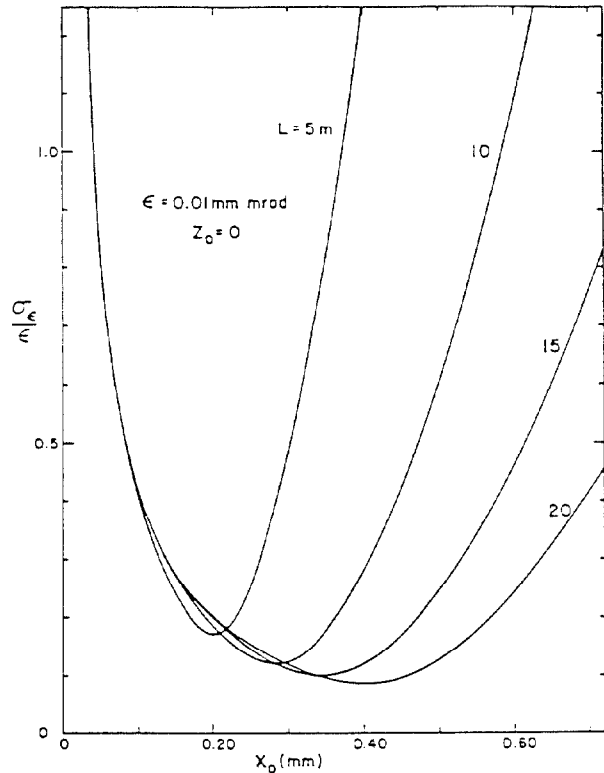


Fig. 2: Precision of emittance measurement  $\sigma_\epsilon$  vs. waist size  $x_0$ , for different profile monitor separations  $L$ . The waist is located at the center monitor ( $z_0 = 0$ ), and  $\epsilon = 0.01$  mm · mrad. The precision of the beam width at each profile monitor is taken to be  $\sigma_{x_i} = 25$   $\mu$ m.

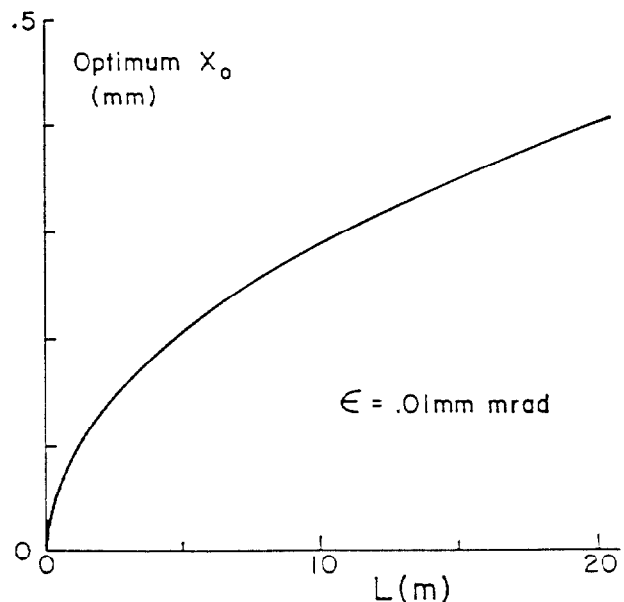


Fig. 3: Waist size  $x_0$  for optimum emittance measurement vs. profile monitor separation  $L$ , for  $\epsilon = 0.01$  mm · mrad.

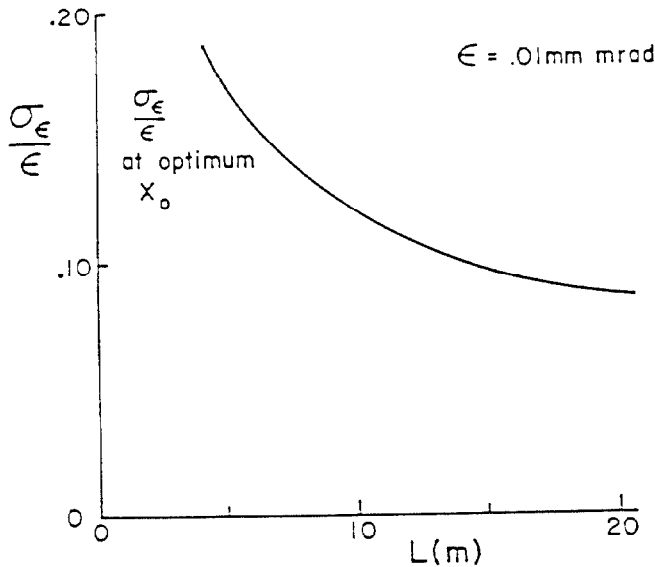


Fig. 4: Precision of emittance measurement  $\sigma_e$  at optimum  $x_0$  and  $z_0$  vs. monitor separation  $L$ , for  $\epsilon = 0.01 \text{ mm} \cdot \text{mrad}$ . The precision of the beam width at each profile monitor is taken to be  $\sigma_{z_i} = 25 \mu\text{m}$ .

All data acquired and calculated are displayed on the MicroVAX workstation. These include plots of the raw data from the wire scanners, along with the fitted profiles. Finally, the beam phase space ellipse at the center scanner is calculated and displayed. Figure 5 shows a sample display. The time needed to acquire a complete set of data depends primarily on the speed of the wire scanners, with the data analysis taking much less time. The scanner speed is a function of several parameters such as the beam repetition rate and the range of scanner motion. Under typical conditions, an emittance measurement is completed in less than one minute.

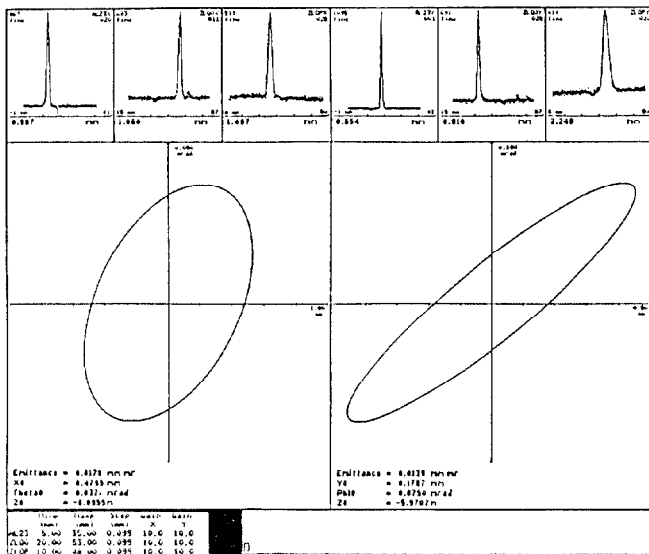


Fig. 5: Sample emittance measuring system display. The horizontal and vertical data are shown on the left and right halves, respectively. The small boxes at the top show beam profile data. The larger boxes show the calculated beam phase space ellipses.

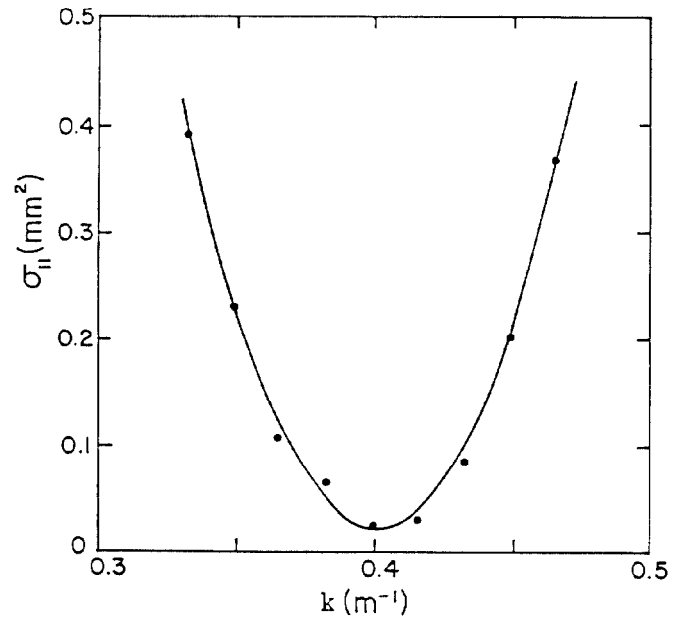


Fig. 6: Square of the horizontal beam size  $\sigma_{11}$  vs. strength  $k$  of a quadrupole singlet 8.03 m upstream from the measurement point. The points are experimental data, and the curve is the best fit parabola.

Preliminary results have been obtained with this system. The three wire scanners are located in a drift space where the beam emerges from the linac. The measured value of the horizontal emittance is  $0.04 \text{ mm} \cdot \text{mrad}$  at a beam energy of 175 MeV, and  $0.02 \text{ mm} \cdot \text{mrad}$  at 250 MeV. This is in good agreement with the expected value of  $10/\gamma \text{ mm} \cdot \text{mrad}$ . In addition, varying the strength of a quadrupole upstream from the emittance measuring system produces the expected rotation of the measured phase space ellipse. Similar results have been obtained in the vertical dimension. The uncertainties in these measurements, both statistical and systematic, are presently under study.

The emittance of the beam has also been measured using a different method.<sup>1</sup> In this technique, the size of the beam is measured at one location, as a function of the strength of an upstream quadrupole. The square of the beam size should have a parabolic dependence on quadrupole strength. Results of such a measurement in the horizontal dimension are shown in Fig. 6. From the parameters of the parabola fit to the data, shown in Fig. 6, the emittance is determined to be  $0.02 \text{ mm} \cdot \text{mrad}$  at 250 MeV, in agreement with the emittance measured using the three scanner technique.

### Summary

Emittance measurements have been made at Bates using an automatic emittance measuring system, consisting of three beam profile monitors equally spaced in a drift region. The results obtained are in good agreement with the values expected at Bates. Measurement of the emittance by an independent technique has yielded similar results.

### References

- [1] M. C. Ross, *et al.*, SLAC-PUB-4278, March 1987.
- [2] R. I. Cutler, J. Owen, and J. Whittaker, Proc. of the 1987 IEEE Particle Accelerator Conference, p. 625, March 1987.
- [3] K. D. Jacobs, *et al.*, "The Beam Profile Measuring System at the Bates Linac," these proceedings.